

Practical Solutions for Reducing Rain-Wind-Induced Vibrations of Cables, in Cables-Stayed Bridges.

Altin SERANAJ

¹Department of Building Construction and Transportation Infrastructure, Polytechnic University of Tirana, Albania

ABSTRACT

Rain vibration of cables is becoming a matter of great concern recently in Japan and other country for design and construction of cables-stayed- bridges. The features of rain vibration are the strong influence of rain on wind-induced oscillation of cable. The cables in cable-stayed bridges, which are stable with respect to wind acting in dry condition, became very unstable with rain, and large amplitude oscillation of cable could be developed under low speed wind. The principal parameters that give a great influence in this phenomenon can be classified in two groups. First the group of the situation of cable were included: the orientation of cable, wind speed, reins intensity. In second group named cables properties were are included natural periods, damping ratio and property of the surface of cables.

In this article is presented only a part of the bibliographic study performed at the Laboratoire Central des Ponts at Chaussee, Paris. This part is focused on two aspects, the mechanism of the problem and the solved solution by surface modification of cables for elimination of this kind of vibrations on the cables. We point here the fact that even many investigation are made this phenomenon is not well known and not yet is found a mathematical model to simulate exactly the real phenomenon.

Here are given only those solutions that tend to stabilise the cable by modification of the surface of the cable. These modifications of the surface of cables tend to “destroy” the water rivulets created on the surface of the cables. Doing so, for every speed and direction of wind and for any rain intensity the water rivulet have not chance to be created on the surface of the cable. These findings are taken from the experiments and investigation on the cables-stayed bridge of Normandy, Paris and cables-stayed bridge of HIGASHI-KOBE, Japan.

INTRODUCTION

Rain vibration of cables is becoming a matter of great concern recently in Japan for design and construction of cables-stayed- bridges. The features of rain vibration are the strong influence of rain on wind-induced oscillation of cable. The cables in cable-stayed bridges, which are stable with respect to wind acting in dry condition, became very unstable with rain, and large amplitude oscillation of cable could be developed under low speed wind around 10m/s. for the first time this phenomena have been seen in the bridge Meiko-Nishi (Japan) and after in the others cable-stayed bridges as: Aratsu, Higashi -Kobe (Japan), Dömitz (Germany), Erasmus (Holland) est.

The name of these phenomena is made from Hikami [1] in 1986 as « Rain-Wind » phenomenon. The same name is also used from Matsumoto in 1988 [2].

Many analytical and experimental investigations have been made for known the influence of different factors that produce this phenomenon in many country. The reason of this article is to make a representation to this phenomenon, to represent some analytical and experimental investigation made by different authors and conclusion yielding from this investigation.

This article is composed on two parts. In the first part is expressed the phenomenon, in second are given some solution that can be used for elimination of vibrations produced from this phenomenon.

1. PRINCIPLE OF EXCITING RAIN-WIND MECHANISMS

Detailed observation of the interaction between the motion of acrylic tube during the model test and the motion of one ore two rivulet on the surface of the tube in the circumferential direction led to finding the new mechanism.

The response of cables subjected to the rain-wind excitation has been with big amplitudes. Menu experimental investigation has been made in wind tunnel including also the rain.

1.1 GENERAL DATA FOR THE EXPERIMENT RAIN-WIND

For the response of the model are used different deviation and inclination angles (this angles α, β are given in figure below). The dimension of the wind tunnel is 2.7m high and 1.8m wide, the maximum speed is about 30m/s. Wind tunnel test is presented on the fig. 1. The diameter of model is the same as the prototype for the reason to eliminate the scale effect of the water rivulet and cable diameter. The cable is inserted inside an acrylic tube with a smooth surface. The position of shower that stimulates the rain can be changed depending the model position. The moment that the response of the model have big amplitude is when on the model is created the water rivulet that move in circumferential direction. For our study the rain intensity used corresponds to the intensity with the biggest amplitude in the model response.

1.2 CROSS SECTION CABLE MODIFICATION

Interaction cable –rivulet is very difficult to be understood because of the complexity. The cross section shape is a function of the water rivulet on the surface of the cable. This position is depended on the wind speed rain intensity, dynamic property of cable, friction force cable-water rivulet.

1.3 ENERGY IMPUT

If the resulting wind force acting on the entire cross section is oscillating at the same frequency an with the same sign as the oscillation frequency of the cable or with a little time lag positive work is done and the oscillation system gets an energy input.. For a generalized system and a harmonic excitation force it can be written as follows for x-direction Eq. (1)

$$W = F \cdot s = \int_t F_x(t) \cdot \dot{x}(t) dt = \int_t \bar{F}_x \sin(\omega t + \mathcal{G}) \cdot \bar{\dot{x}} \sin(\omega t) dt \quad (1)$$

$W \rightarrow$ Energy input respectively, $F_x(t) \rightarrow$ Force component acting parallel to the momentary vibration velocity $[N]$, $\bar{F}_x \rightarrow$ Amplitude --, $[N]$, $\dot{x}(t \rightarrow)$ Momentary vibration velocity $[m/s]$, $\bar{\dot{x}} \rightarrow$ Amplitude of --, $[m/s]$, $\omega \rightarrow$ Natural angular frequency of the structure $[rad/s]$, $\mathcal{G} \rightarrow$ Angle of phase difference between $F_x(t)$ and $\dot{x}(t)$

In the figure 2 – 4 this energy is presented with the dark color.

1.4 EXCITATION MECHANISM

Essentially three types of mechanisms have been observed. They are characterized by the location of the rivulet on the cross section and the vibration direction of the cable. Fig 2-4 show the time history of the following five parameters during two oscillation period.

1 → Deflection of the cross section.

2 → oscillation acceleration.

3 → force caused by the rivulet (neglecting turbulence and Karman vortices) in wind direction ΔF_x , in cross-wind direction F_y fig.3 and F_x in fig.4

4 → oscillation velocity

5 → Energy input caused by the rivulets $F_x(t) \cdot \dot{x}(t)$ (or) $\dot{y}(t)$

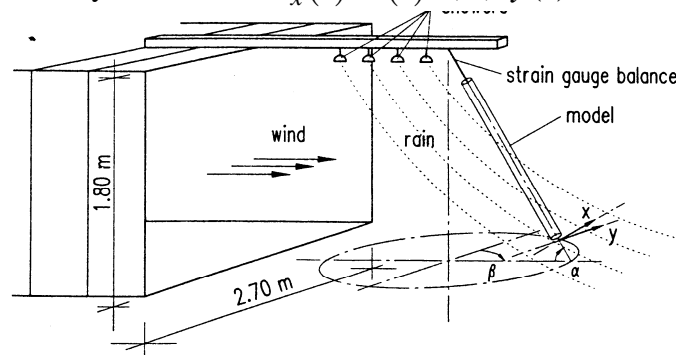


Fig.1 Wind tunnel test (inclination and deviation angle)

MECHANISM 1(Oscillation in wind direction)

This mechanism is presented in the figure 2. The movement of rivulets is symmetric. This rivulet is behind the meridian 90° . The biggest amplitude for this mechanism is for the inclination angle $\alpha = 30^\circ$, deviation angle $\beta = +90^\circ$ and for win speed $V = 22m/s$.

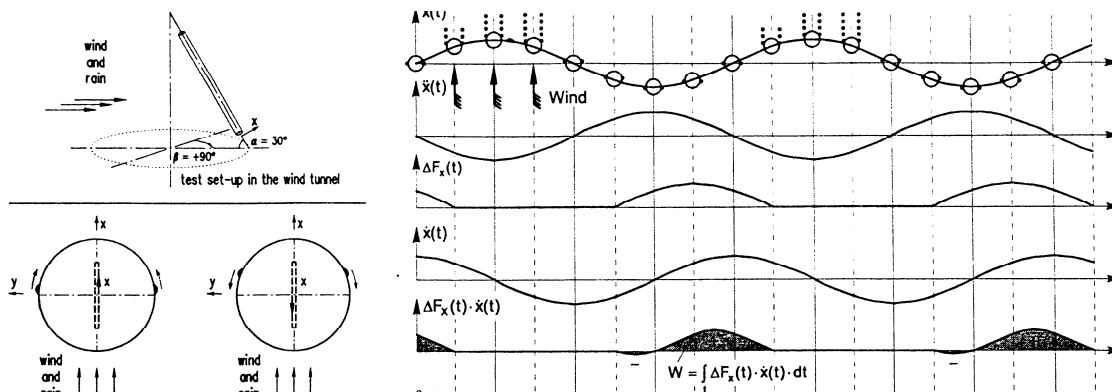


Fig.2 Input energy for first mechanism $\alpha = 30^\circ$, $\beta = +90^\circ$, $V = 22m/s$

MECHANIZM 2(cross-wind vibration two rivulet)

The rivulets are in front of the meridian 90° and movements of rivulet are not symmetrical. This type of rain-wind-induced vibration can occur in cables inclined against the wind direction. At a sufficient wind speed the rivulet on the underside of the cable is divided into two lateral rivulets shortly in front of the lateral 90° . Due a stochastic initial lateral motion of the cable, one of the rivulet is shifted into the 90° position, whereas the other rivulet move toward the stagnation point. Because these cross sections shape the pressure distribution becomes asymmetrical and causes a lateral force F_y .

MECHANIZM 3(cross-wind vibration one rivulet)

The rivulet is now after the meridian (fig.4). This mechanism is presented for the cable with the angles $\beta = \pm 45^\circ$ and $\alpha = 30^\circ$. This mechanism is produced for low wind speed. For higher speed is produced the mechanism 1, 2.

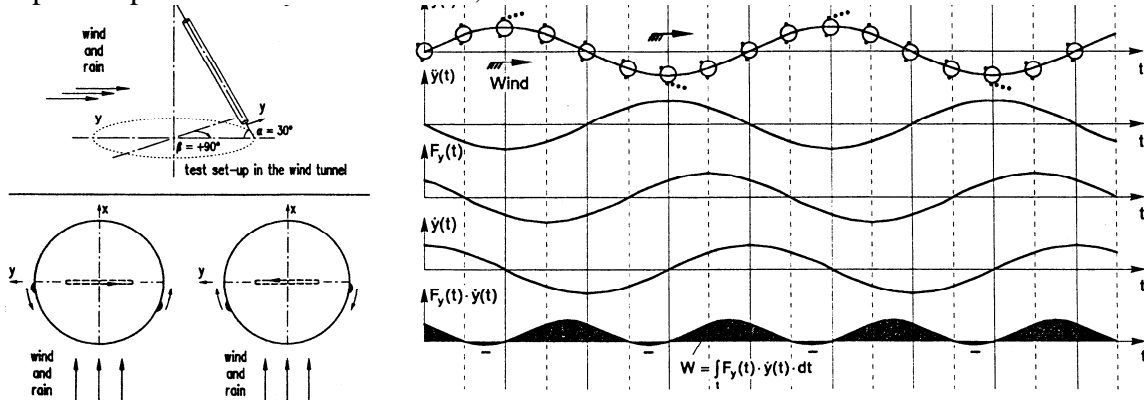


Fig.3 Input energy for second mechanism $\alpha = 30^\circ, \beta = +90^\circ, V = 18m/s$

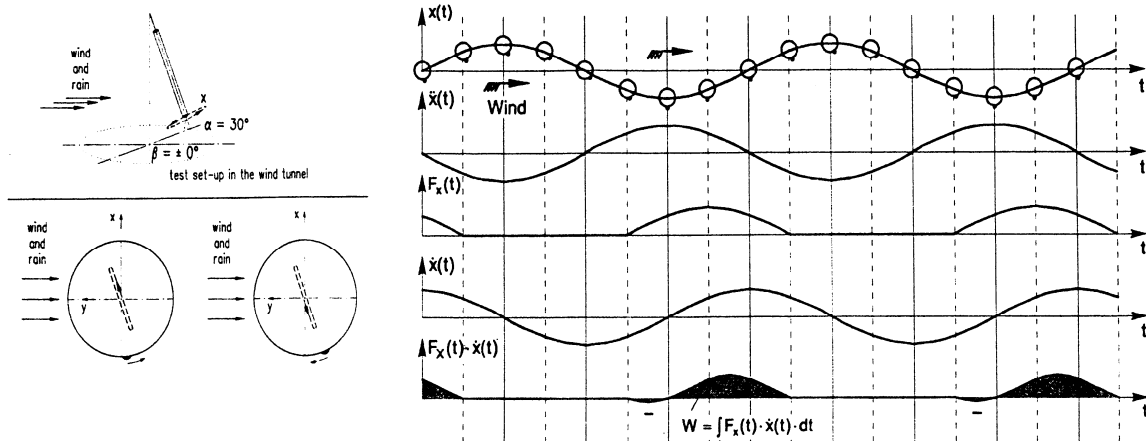


Fig.4 Input energy for third mechanism $\alpha = 30^\circ, \beta = +0^\circ, V = 19m/s$

The vibration are produced for wind speed $V \in [5 \div 25]m/s$ and for the frequencies low than $8.9Hz$. However, at these frequency only-rain-wind-induced amplitudes of the magnitude of the vortex excited amplitudes arose. At higher frequencies, increasing vibration acceleration makes the water, due to its masse of inertia unable to follow the motion of the cable. That could be the reason for low amplitude for high frequencies. For inclined cable the largest amplitudes occurred at the angles $\beta \pm 45^\circ$.

2. AERODYNAMIC RESPONSE OF PE STAY CABLES WITH DIFERENT SURFACE ROUGHNES

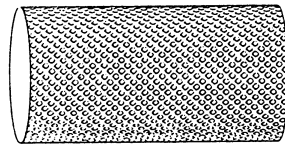
The test are made for different pattern surface presented on fig 5. The model $A_1 - A_6$ have a uniform pattern. For the models $B_1 - B_3$ and models C_2, C_3 is applied a pattern surface as given by the figure below. The characteristics of this model are given in the table. For the models A_i, B_j is used the wind tunnel with 2m height and 1m width. Wind speed $V = 25m/s$ that correspond to the Reynolds number $Re = 2.2 \cdot 10^5$. Wile for the models C_k dimension tunnel are 3m and 2m and the maximum speed is used $V = 55m/s$.

Tab.1 Mode A_i, B_j, C_k

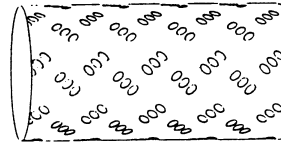
Model	Diameter D (m)	Surface roughness (μm)	Relative surface roughness (k/D)
A ₁	0.1315	3	2.3×10^{-5}
A ₂	0.1220	30	2.5×10^{-4}
A ₃	0.1315	100	7.6×10^{-4}
A ₄	0.1235	200	1.6×10^{-3}
A ₅	0.1240	600	4.8×10^{-3}
A ₆	0.1275	1,500	1.2×10^{-2}
B ₁	0.1465	200	1.6×10^{-3}
B ₂	0.1465	600	4.1×10^{-3}
B ₃	0.1490	1,200	8.1×10^{-3}
C ₁	0.140	3	2.1×10^{-5}
C ₂	0.140	1,500	1.1×10^{-2}
C ₃	0.140	1,500	1.1×10^{-2}

Remarks

smooth
 uniform distribution
 “
 “
 grid-like pattern all over surface
 smooth
 discrete concave patterns



B₃ Model



C₂ Model

Fig.5 Surface pattern for models

The drag coefficient of a body with a circular section and smooth surface in a uniform flow is a function of the Reynolds number, $Re = \frac{V \cdot D}{\varrho}$

$V \rightarrow$ wind speed, $D \rightarrow$ cable length, $\varrho \rightarrow$ kinematics' viscosity

This means that the flow around the body changes with Reynolds number.

Surface roughness causes a shift in the separation point along the body were the section is circular and this accelerate the transition in top the turbulent flow region.. Since change in drag coefficient is dominated by the location of the separation point the surface roughness also has a great effect on the drag coefficient in the range of Reynolds number.

Figure 6 through 9 show measured drag coefficients for the various models. All of this drag coefficient is nearly 1.2 in the sub critical range. from figure 6 and 7 it is evident that in the case of cables with a uniformly distributed surface roughness, the critical Reynolds number drops as the surface roughness increases. With increasing the relative surface roughness k/D, the drag coefficient at the critical Reynolds number exceeds the drag coefficient of the smooth round cable models by 0.5. With increasing wind velocity, the drag coefficient increases and has a tendency to rapidly approach 1.2. For model A6 which has a uniform relative surface roughness of about 1% of its diameter the drag coefficient are about 0.9 and 1.2 at the critical Reynolds number. Figure 8 show the drag coefficient for models Bi which have the same degree of roughness as the model A4, A5 and A6 but in a grid-like pattern. In this case the increase of the drag coefficient increase gradually with increasing of wind velocity.

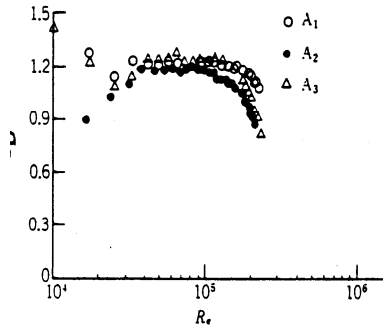


Fig.6 Drag coefficient-Reynolds number relation $A_1 - A_3$

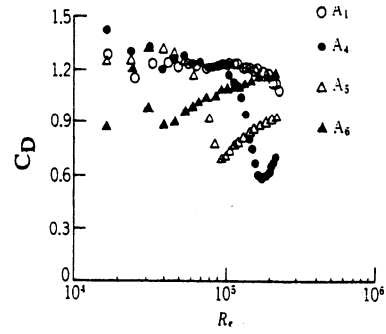


Fig.7 Drag coefficient-Reynolds number relation $A_4 - A_6$

Figure 9 shows the drag coefficients of models C_i . Which have approximately the same degree of surface roughness as the model A6 and B3 but applied discretely. Both C2 and C3 have the same behaviour. The critical number and drag coefficient are $R_e = 1 \cdot 10^5$ and $C_t = 0.6$ respectively. With the range of Reynolds number $R_e = 5.5 \cdot 10^5$ that corresponds to the wind velocity $V = 55m/s$ the drag coefficient remains constant.

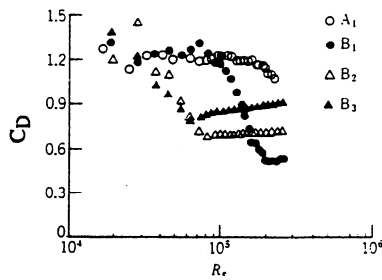


Fig.8 Drag coefficient-Reynolds Number relation $B_1 - B_3$

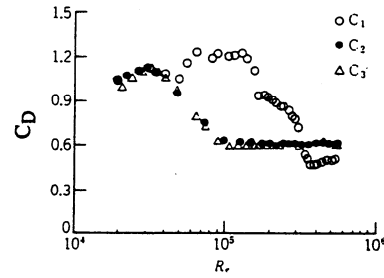


Fig.9 Drag coefficient-Reynolds number relation $C_1 - C_3$

So, equivalent Drag coefficient can be obtained with discrete roughness patterns as with smooth surfaces within the design wind velocity.

2.1 INFLUENCE OF SURFACE ROUGHNES FOR ELEMENATION OF THE VIBRATION RAIN-WIND

Figure 10 show the wind tunnel apparatus used. Models C_1 and C_3 with the length 3m are used for the test. The model was freely fixed on springs in the direction perpendicular the cable axis. Model weight was 194N, natural frequency about 1.8Hz, the logarithmic structural damping ratio ranged from 0.003 to 0.004 and the Scruton number $1.7 \div 2.3$. Table 2 show the experimental parameters for each cable with inclination angle $\alpha = 45^\circ$ and deviation angle $\beta = 45^\circ$. These experiments were done in an Eiffel type wind tunnel having a 2.5m height and 1.5m width and equipped with a water nozzle.

Tableau 2 Model dimensions

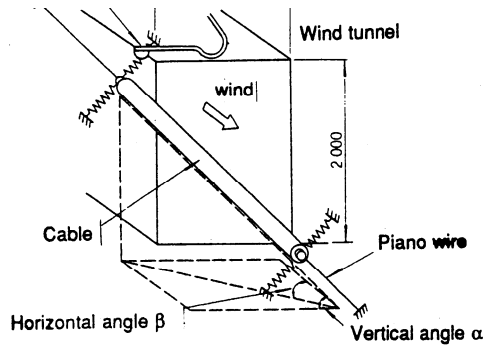


Fig.10 Model fixation

Model	Weight per length (N/m)	Frequency (Hz)	Logarithmic decrement δ	Remarks
C ₁	64.7	1.8	0.0035	Smooth
C ₂	64.7	1.8	0.0039	Discrete concave pattern
C ₃	64.7	1.8	0.0032	Discrete convex pattern

VIBRATION RESPONSE DURING RAINFALL

With simulated rainfall at water volume of 0.8 , 1.4 and 2 l/min., for model C₁ vibration occurred at wind velocities of about 9÷12m/s. This is a characteristic already proved at past experiments Figure 11 shows the damping characteristics of cables at a vibration amplitude ratio A/D of 0.1. Of the three water volume studied, figure 8 makes clear that the wind velocity range in which rain vibration occurred was the widest and negative damping largest with a water volume of 8 lit/min. The maximum logarithmic decrement for this cable model is 0.07. Unstable vibration occurred when the reduced wind velocity V/fD exceeded about 40.

For models C₂ and C₃ with roughened surfaces no rain vibration occurred as shown in the fig 12. for these models the other intensity water is used but no vibration occurred.

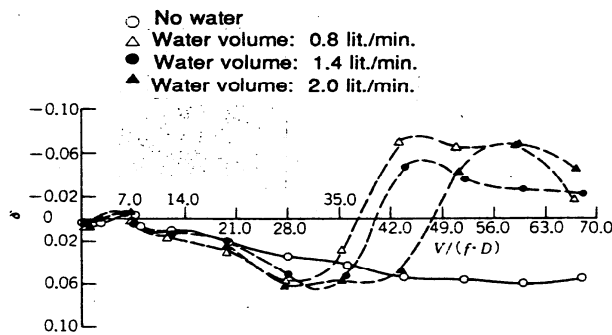


Fig.11 Damping characteristics of model C₁

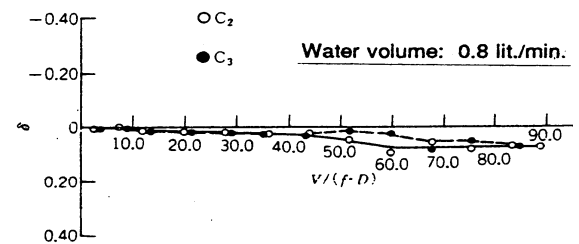


Fig.12 Damping characteristics for the model C₂ and C₃

3. ELEMINATION RAIN-WIND VIBRATION SOLUTION USED

We have show the principal vibration that influence in the response of the cables subjected to this excitation.

This are : wind speed, cable orientation, rain intensity, cable characteristics as natural frequency, damping, cable roughness etc. Based in the result of many analytical and experimental investigation we are giving here same example that are used in al cables stay bridges. Sam of this bridges have been firstly subjected to this type of excitation.

3.1 SURFACE MODIFICATION

This solution is used in the Normandy bridge (France). As the experiment shows that is very important to “destroy” the water rivulet running on the surface cable. In Fig 13 is presented the surface cable modification that can “destroy” this water rivulet.

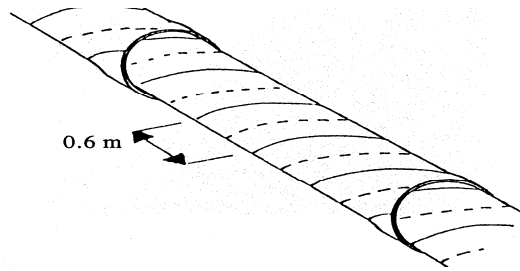


Fig.13 Cable Surface modification used for Normandy Bridge, France

Filets with dimensions 1.3mm high and 2mm large are fixed in a helicoidally way on the surface of the cable.

3.2 AERODYNAMICS METHOD OF CABLE VIBRATION CONTROL

By the resultants of the experiment that show as the influence of the turbulence, (this investigation is made during the study for solving the rain-wind vibration subjected to the cables-stayed bridge of HIGASHI-KOBE, Japan. One solution is found. This is given in fig 14 and consist in longitudinal parallel surface projection. These make the turbulence flow that makes the creation of water rivulet mechanism impossible. After made on place of this solution and investigation during 3 years not vibration occurred in the cables.

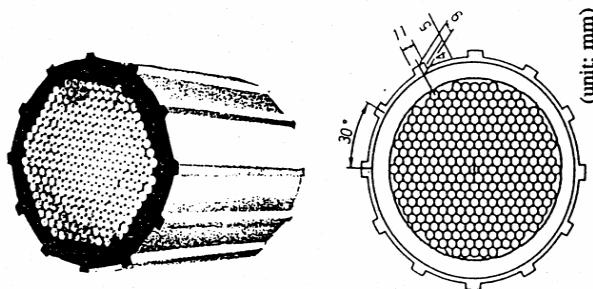


Fig.14 Higachi-Kobe cable stayed bridge aerodynamic solution

CONCLUSIONS

- Interaction between the rivulet in circumferential direction and the vibration of the cylinder is fundamental for the excitation rain-wind
- The instability can be for this condition $\beta = \pm 45^\circ$. The wind speed is around the interval $5 - 25m/s$.
- The circumferential oscillation of the upper rivulet is coupled with the vertical oscillation of the cable and is indispensable to the growth of rain vibration.
- The practical solution by modification of the surface of the cables for “destroying” the water rivulet that may be caused in a range of combination of wind and rain have been proven to be a good solution

REFERENCES

- [1] Hikami, Y. (1986). « Rain Vibrations of cables of A Cable Stayed Bridge. » J. Wind Engineering (Japan), No. 27, pp.17-28 (in Japanese).
Langsoe, H.E. and Larsen, O.D. (1987). « Generating Mechanism for Cable Oscillation at the Faroe Bridge. » Proc. Int. Conf .on Cable Stayed Bridges, Bangkok, pp 18-20.
- [2] Matsumoto, M.,Shiraishi, N., Kitazawa, M., Knisely, C.W.,Shirato, H., Kim, Y. and Tsujii, M. (1988a). « Aerodynamic Behavior of Inclined Circular Cylindres - Cables Aerodynamics.» Proc. Int. Colloquium on Bluff Body Aerodynamics and its Applications, 17-22 Oct.,Kyoto,Japan
- [3] M. Matsumoto « Cables vibration and its Aerodynamic/Mechanical Control », Proc. Of Cable-stayed and Sunspension Bridges, Deauville, 1994, pp439-452.
- [4] Verwiebe, C. Rain-Wind-Induced Vibrations of Cables and bars. Proceedings Int, Symposium on Advances in Bridge Aerodynamics, Ship Collision Analysis and Operation and Maintenance, 10-13 May 1998, Technical Univ. Of denmark, Lyngby, Denmark,1998.
- [5] Y. Higami - Rain vibration of cables on cable-stayed bridge - Jour. Of Wind Eng. No. 27, 1986.